Actual Circuit Verification of LC Series Resonant Converter with Power Factor Control for Effective Power in Load regulation

Akito Nakagaki
Graduate school of natural science and technology
Okayama University
Okayama, Japan
pr3g4r2e@s.okayama-u.ac.jp

Eiji Hiraki
Graduate school of natural science and technology
Okayama University
Okayama, Japan
hiraki@okayama-u.ac.jp

Kazuhiro Umetani
Graduate school of natural science and technology
Okayama University
Okayama, Japan
umetani@okayama-u.ac.jp

Ishihara Masataka
Graduate school of natural science and technology
Okayama University
Okayama, Japan
masataka.ishihara@okayama-u.ac.jp

Yuto Yoshimura
Graduate school of natural science and technology
Okayama University
Okayama, Japan
pqx88wuy@s.okayama-u.ac.jp

***Abstract*—Resonant converters are poor stability about load reguration. New control methods have been proposed to stabilize resonant converters versus load variations. This paper describes the LC series resonant converter using a power factor control with stable control characteristic for load regulation. The proposed control adjusts the power factor that determined by primary current and voltage. Previous research proposed phase shift control method for power factor. This method controls the power factor by using the voltage across the resonant capacitor. The problem with this method is that it assumes the resonant capacitor voltage is sinusoidal when controlling the power factor. Therefore, power factor control becomes more difficult when the waveform is distorted. This research proposed a new power factor control method to address this problem in simulations. Hence, this paper shows that the proposed method has stable control characteristic versus load regulation even in actual circuits.**

***Index Terms*—LC series resonant converter, buck converter, power factor control, load regulation**

I. Introduction

Recently, data centers have been demanding high power conversion [1]–[3]. Fig. 1 shows an example of a server system in the future [1]. This system demands higher efficiency and higher power density. One method to achieve higher power density in this system is to increase the frequency. It is possible to reduce the size of the passive elements. This system can reduce the volume of the system to achieve higher power density. The literature [1] indicates that the most efficient system among the various distribution systems is the 400 V DC high voltage distribution system. To achieve this system, each converter of server rack need to be optimized for high efficiency. This paper focuses on the converter (Point of Load) before CPU, memory, and other loads. The POL converter need to be stability versus load regulation because depending on usage load value vary.

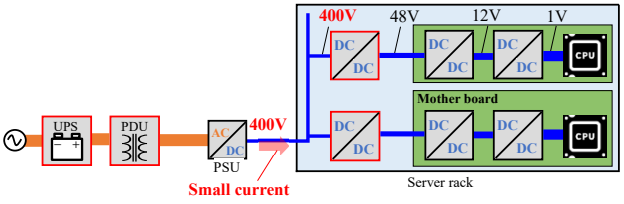

Fig. 1. Server system

The POL converter is buck converter in present. Fig. 2 shows a diagram of the buck converter. The buck converter controls the output voltage by adjusting the supply energy in the inductor. Hence, The output voltage of the buck converter doesn't depends on the load. In the plant transfer function, the output load is handled as a damping factor. The stable control characteristics can be achieved versus load fluctuations since the crossover frequency does not change. However, the buck converter is generally are unsuitable for operating high frequency since to control duty ratio(Pulse Width Modulation(PWM)). It is difficult for the buck converter to maintain a low duty ratio at higher frequency. Therfore, achieving the mentioned high efficiency and high power density is difficult.

This paper assumes to replace buck converter with a resonant converter. Resonant converters easily achieve soft switching for high efficiency [4]–[6]. Furthermore, the reduction of passive elements volume due to often drive high frequency. This paper focuses on LLC converter that can easily achieve mentioned above and compose few number of parts is shown

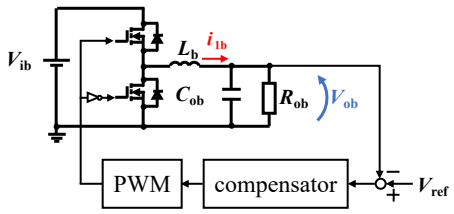

Fig. 2. Buck converter

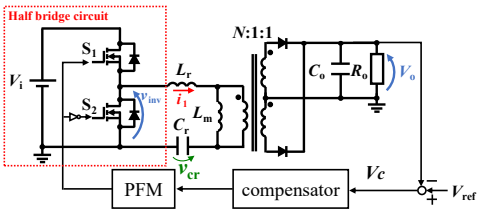

Fig. 3. LLC converter

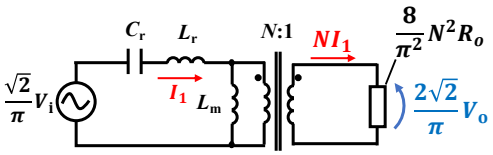

Fig. 4. Fundamental harmonics analysis for LLC converter

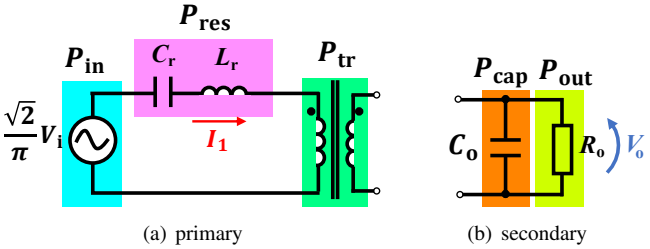

Fig. 5. Simplified LC series resonant converter for power relationship

Fig. 3. Applying the LLC converter to a POL converter is not simple. Because, the transfer function of the plant depends on the load, which is different from the buck converter [7].

Previous research proposed power factor control to improve this issue [8], [9]. Proposed method controls power factor, which consists of the primary current i_1 and primary voltage v_{inv}. The buck converter controls output voltage by adjusting supply energy in the inductor. previous research has considered this control method as an important key for obtaining stability versus load vary. Proposed method controls supply energy for the resonant tank in the LLC converter. Hence, mentioned issue can solve that the control method of the LLC converter replace proposed method. In contrast to PFM, the frequency is automatically determined after the power factor is determined. Previous research has reported on the effectiveness of the proposed method [8], [9]. Proposed theory for power factor control is based on fundamental harmonics analysis (FHA) shown in Fig. 4. the condition that the resonant current and voltage are sinusoidal due to the complexity of the theoretical equation. Proposed method that phase shift power factor control has been verified to work with an LC series resonant converter [9]. However, the phase shift power factor control is difficult to work in un-sinusoidal. Therefore, previous research prposed power factor control for effective power [8]. This method is feasible in un-sinusoidal resonant voltage and current. The effectiveness of the proposed method has been reported only in simulation in LC series resonant converters. This paper confirms with an LC series resonant converter that stable control characteristic can be obtained versus load variations even in actual circuit. Note that, this paper refers power factor control for effective power as proposed method.

II. The Method of the Power Factor Control

A. The state space equation of power factor

This section describes that state space equations of power factor control and buck converter are equivalent. Fig. 5 shows simplified LC resonant converter. The state space equation of power factor control derive from each power relationship shown in Fig. 5. The primary power relationship is expressed as (1). Note that P_{in} equals input power, P_{res} equals resonant tank power, P_{tr} equals transformer power.

$$P_{\mathrm{in}} = P_{\mathrm{res}} - P_{\mathrm{tr}} \tag{1}$$

All the energy in the resonant tank supply to the inductor when the current I_1 is at maximum. The reason, capacitor voltage is at zero when current is at maximum. Therefore, it can be replaced as in (2). Note that N winding ratio.

$$\frac{\sqrt{2}}{\pi}V_{\mathrm{i}}I_1\cos\theta - \frac{\mathrm{d}}{\mathrm{d}t}\left(\frac{1}{2}L_{\mathrm{r}}(\sqrt{2}I_1)^2\right) = \frac{2\sqrt{2}}{\pi}NV_{\mathrm{o}}I_1 \tag{2}$$

Assuming that the primary transformer power supply directly to the secondary, the equation becomes (3)

$$\begin{aligned} P_{\mathrm{tr}} &= P_{\mathrm{cap}} - P_{\mathrm{out}} \\ \frac{2\sqrt{2}}{\pi}NV_{\mathrm{o}}I_1 - \frac{\mathrm{d}}{\mathrm{d}t}\left(\frac{1}{2}C_{\mathrm{o}}V_{\mathrm{o}}^2\right) &= \frac{V_{\mathrm{o}}^2}{R_{\mathrm{o}}} \end{aligned} \tag{3}$$

Previous research derived state space equation as shown in (4) based on equation (2), (3). This paper omits Details of the derivation because previous research indicates. The state space equation of buck converter also shows (5), refer to the literature [10], [11] for more details.

$$\begin{aligned} \frac{d}{dt}\begin{pmatrix} I_1 \\ V_{\mathrm{o}} \end{pmatrix} &= \begin{pmatrix} 0 & -\frac{\sqrt{2}N}{\pi L_{\mathrm{r}}} \\ \frac{2\sqrt{2}}{\pi C_{\mathrm{o}}} & -\frac{1}{C_{\mathrm{o}}R_{\mathrm{o}}} \end{pmatrix}\begin{pmatrix} I_1 \\ V_{\mathrm{o}} \end{pmatrix} \\ &+ \begin{pmatrix} \frac{\sqrt{2}N}{\pi L_{\mathrm{r}}} \\ 0 \end{pmatrix}\frac{V_{\mathrm{i}}}{2N}\cos\theta \end{aligned} \tag{4}$$

$$\begin{aligned} \frac{d}{dt}\begin{pmatrix} I_{1\mathrm{b}} \\ V_{\mathrm{ob}} \end{pmatrix} &= \begin{pmatrix} 0 & -\frac{1}{L_{\mathrm{b}}} \\ \frac{1}{C_{\mathrm{ob}}} & -\frac{1}{C_{\mathrm{ob}}R_{\mathrm{ob}}} \end{pmatrix}\begin{pmatrix} I_{1\mathrm{b}} \\ V_{\mathrm{ob}} \end{pmatrix} \\ &+ \begin{pmatrix} \frac{1}{L_{\mathrm{rb}}} \\ 0 \end{pmatrix}V_{\mathrm{ib}}D \end{aligned} \tag{5}$$

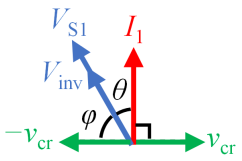

Fig. 6. Vector diagram of waveform in phase shift control.

Comparing the state space equations of the buck converter and power factor control are similar. Based on this equation, transfer function of power factor have also derived in previous research [12]. Transfer function of power factor control has been shown to be similar to the buck converter as well. Therefore, power factor control can be expected to provide stable control characteristic versus load vary.

B. The phase shift power factor control

Fig. 7 shows the waveform of the phase shift power factor control. The previous method generates triangle waveform V_{saw} based on the zero-crossing point of the resonant capacitor voltage v_{cr}. That controls the phase angle φ by comparing the triangle waveform V_{saw} with the output of the comparetor V_{c}. The phase angle of power factor θ is determined by the current i_1 and voltage v_{inv}. The previous method indirectly controls the phase angle θ as (6) and Fig. 6.

$$\theta = 90 - \varphi \tag{6}$$

Replacing the phase φ with the amount of phase shift T_φ is expressed as (7).

$$T_\varphi = \left(1 - \frac{\cos^{-1}(V_{\mathrm{c}})}{90[\mathrm{deg}]} \times \frac{T}{4}\right) \tag{7}$$

Since the calculation of $\cos^{-1}(V_{\mathrm{c}})$ is difficult on the actual circuit, it is simplified as (8).

$$T_\varphi = V_{\mathrm{c}} \times \frac{T}{4} \tag{8}$$

The previous method has difficulty in handling unsinusoidal resonant capacitor voltage v_{cr}. The shape of the waveform cannot be determined from the zero-crossing point of the resonant capacitor voltage v_{cr}. Furthermore, this method assumes the waveform of sinusoidal when calculating the phase angle φ. The resonant capacitor voltage v_{cr} becomes increasingly distorted under light load conditions. The power factor control method for addressing waveform distortion will be described in the next section.

C. The Power factor control for effective power

This section describes How to implement power factor control for effective power. proposed method control the power factor by reading the instantaneous voltage of the resonant capacitor voltage to estimate the power factor and then adjusting the effective power. The duty ratio of the half bridge circuit fix

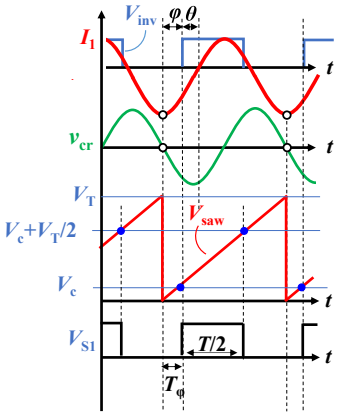

Fig. 7. Operating waveform of previous method

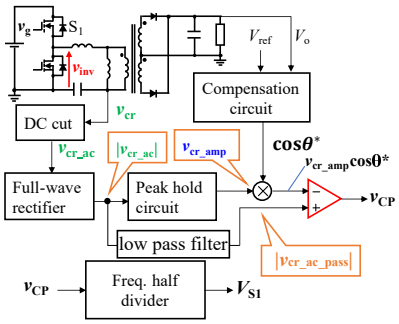

Fig. 8. Simplefied control circuit of proposed method

at 0.5. The output voltage of the half bridge circuit is ecpressed as (9).

$$v_{\mathrm{inv}}(t) = \begin{cases} V_{\mathrm{i}} & (0 \le t < T/2) \\ 0 & (T/2 \le t < T) \end{cases} \tag{9}$$

Therefore, effective power is expressed as (10).

$$P_{\mathrm{i}} = \frac{V_{\mathrm{i}}}{T} \int_0^{\frac{T}{2}} i_1(t)dt \tag{10}$$

the primary current i_1 flow in the capacitor can be expressed as i_1=$C_{\mathrm{r}}(dv_{\mathrm{cr}}(t)/dt)$. Substitute this expression into that (10).

$$P_{\mathrm{i}} = \frac{V_{\mathrm{i}}C_{\mathrm{r}}}{T} \int_0^{\frac{T}{2}} dv_{\mathrm{cr}}(t) = \frac{V_{\mathrm{i}}C_{\mathrm{r}}}{T}\{v_{\mathrm{cr}}(T/2) - v_{\mathrm{cr}}(0)\} \tag{11}$$

resonant capacitor voltage of AC component depends on the output voltage v_{inv} of half bridge circuit. After half period is same absolute value since duty ration 0.5.

$$v_{\mathrm{cr}}(T/2) = -v_{\mathrm{cr}}(0) \tag{12}$$

substituting (12) into (11) is expressed as (13).

$$P_{\mathrm{i}} = -2V_{\mathrm{i}}C_{\mathrm{r}}\frac{v_{\mathrm{cr}}(0)}{T} \tag{13}$$

Next, to find apparent power S_{i}. This paper considers that Amount of all charge flowing into the resonance tank is apparent power. So, the apparent power regards as the voltage

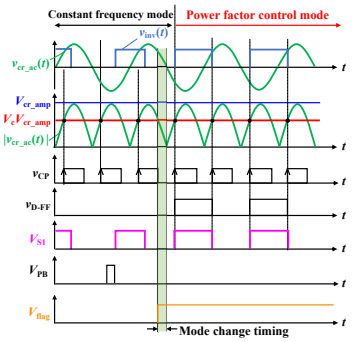

Fig. 9. Operating waveform of proposed method

of the maximum value of the capacitor $V_{\mathrm{cr\_amp}}$. Then, apparent power is expressed as (14).

$$S_{\mathrm{i}} = 2V_{\mathrm{i}}C_{\mathrm{r}}\frac{V_{\mathrm{cr\_amp}}}{T} \tag{14}$$

The power factor $\cos\theta$ can be expressed as (15) from (13) and (14).

$$\cos\theta = \frac{P_{\mathrm{i}}}{S_{\mathrm{i}}} = \frac{-v_{\mathrm{cr}}(0)}{V_{\mathrm{cr\_amp}}} \tag{15}$$

From the above equation, the proposed method can control power factor $\cos\theta$ to monitor the voltage of the resonant capacitor $v_{\mathrm{cr}}(0)$ at the moment when the high-side switch S1 of the half bridge circuit is turned on, and the instantaneous maximum voltage $V_{\mathrm{cr\_amp}}$. The control value $cos\theta$ replaces the voltage of the compensator V_{c} to obtain (16).

$$v_{\mathrm{cr}}(t) = V_{\mathrm{c}} \times V_{\mathrm{cr\_amp}} \tag{16}$$

The proposed method controls the total power factor, whereas the previous method controls the fundamental wave power factor. Therefore, the previous methods will exhibit worse control characteristics than the proposed method under unfavorable circuit conditions. Additionally, these previous methods will show slower load response speed compared to the proposed method in the same conditions.

III. Implement Control Circuit

This cahpter describes about the control circuit of the proposed method. Fig. 8 shows the simplified control circuit for proposed method. Then, Fig. 9 shows the operating waveform for the proposed method.

A. Control circuit for detecting resonant capacitro voltage

Fig. 10 shows LC series resonant converter and control circuit for detecting resonant capacitro voltage. Detecting the resonant capacitor voltage v_{cr} by connecting the detection capacitor in series with the resonant capacitor. Because the control circuit needs to attenuate the voltage to operate correctly. Then, a bandpass filter circuit is inserted to cancel the DC component of the resonance voltage. Resonance capacitor voltage v_{cr} is positively and negatively symmetrical, so rectification can simply detect voltages $v_{\mathrm{cr}}(0)$ and $v_{\mathrm{cr}}(T/2)$.

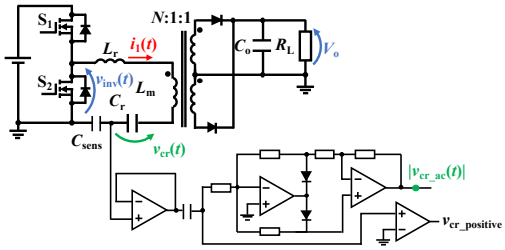

Fig. 10. Series resonant converter and control circuit for detecting resonant capacitor voltage

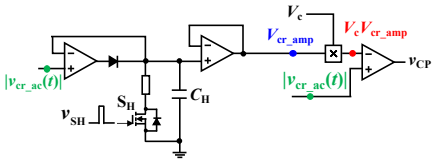

Fig. 11. Peak hold circuit and multiplier

Note that the control circuit uses absolute circuit for rectifier. The absolute circuit using the op-amp is not affected by voltage drop at the diodes.

At the moment when switch S1 is turned on, the resonant capacitor voltage should be negative, as indicated in (16). Therefore, the comparator generates the voltage $V_{\mathrm{cr\_positive}}$ to determine whether the voltage across the resonance capacitor is positive or negative. The resonant capacitor voltage changes each cycle before stabilizing into a steady state.

B. detecting maximum resonant capacitor voltage and multiplier

Fig. 11 shows peak hold circuit and multiplier. The capacitor of the peak hold circuit C_{H} stores and holds the rectified resonant capacitor voltage $|v_{\mathrm{cr\_ac}}|$. Therefore, a monostable multivibrator turns on the peak hold circuit switch at the moment when the high-side switch is turned off, allowing for a discharge period. The multiplier multiplies the maximum voltage value of the resonant capacitor $V_{\mathrm{cr\_amp}}$ and the output voltage compensator V_{c}. Then, the comparator compares this multiplied voltage with the rectified resonant capacitor voltage $|v_{\mathrm{cr\_ac}}|$. This process generates the switching pulses that control the on and off of the high-side switch.

C. Generating gate signal circuit

Fig. 12 shows the generating gate signal circuit. As shown Fig. 12, each rising edge of the switching pulse corresponds to the on or off operation of the high-side switch. the use of an AND circuit and a flip-flop circuit to generate the gate signals. The generated signal is transmitted to the half-bridge circuit.

D. Startup power factor control circuit

Fig. 13 shows startup circuit. The proposed method generates a gate signal using the output voltage of the compensator V_{c} and the voltage across the resonant capacitor v_{cr}. At the startup of the Series resonant converter, the control circuit can not generate the gate signal because the resonant capacitor

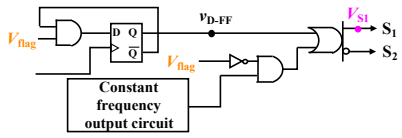

Fig. 12. Generating gate signal circuit

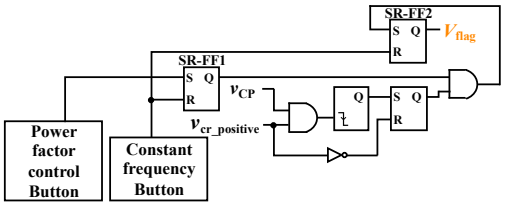

Fig. 13. Startup power factor control circuit

voltage remains unstable and small. At startup, the system must use a control method that is independent of the resonant capacitor voltage v_{cr}. The system adopts how to drive at a fixed frequency. A switch allows switching between two modes: power factor control and fixed frequency operation. Initially, the system increases the input voltage in fixed frequency mode and the switching pulse v_{CP} is generated when the resonant capacitor voltage stabilizes and increases to a sufficient level. At this timing, a voltage V_{flag} is output by pushing the button switches the system to power factor control mode, allowing for stable operation.

IV. Verification of the Actual Circuit for the Proposed Method

This chapter presents the results of experiments conducted on the actual circuit to evaluate the open-loop characteristic of the proposed method. First, indicate the condition of the actual circuit. Second, Describe the amount of delay on the actual circuit. Finaly, The differences from previous studies will be discussed using the experimental results on control characteristics and load response speed.

A. Condition of the actual circuit

Fig. 14 shows schematic of the actual circuit. Table. I shows elements constant. Fig. 15 indicates actual LC series resonant converter and control circuit. In addition, the transfer function of power factor control circuit is expressed as (17). The load is modeled as a current source to derive (17). The reason is the complexity of the derivation process. This paper evaluates behavior based on the theoretical formula (17). In practice, the load resistance is expressed as a damping coefficient, which can lead to deviations between experimental results and theory.

Note that, $e^{-st_{\mathrm{p}}}$ is the amount of delay. The transfer function of power factor control does not include a part of $e^{-st_{\mathrm{p}}}$.

$$\frac{dV_{\mathrm{o}}}{d\cos\theta} = \frac{V_{\mathrm{i}}}{2N} \frac{C_{\mathrm{o}} r_{\mathrm{c}} s + 1}{\frac{\pi^2}{4N^2} L_{\mathrm{r}} C_{\mathrm{o}} s^2 + (\frac{\pi^2}{4N^2} r_{\mathrm{L}} + r_{\mathrm{c}}) C_{\mathrm{o}} s + 1} e^{-st_{\mathrm{p}}} \quad (17)$$

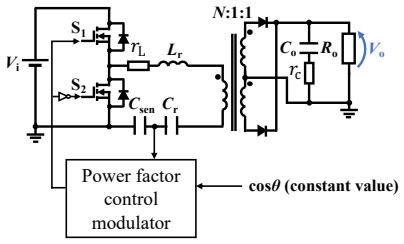

Fig. 14. Actual sereas resonant converter circuit

TABLE I
Sereas Resonant Converter Constant

Resonant inductor L_{r}	20 μH
Parastic resistance of inductor r_{L}	0.5 Ω
Resonant capasitor C_{r}	154 nF
output capacitor C_{o}	240 μF
Parastic resistance of output capacitor r_{c}	0.5 Ω
Sensing capacitor C_{sen}	2.2 μF
Ratio of number windings N	1

B. Delay measurement experiment

This chapter describes delay of proposed method. The amount of delay does not affect the gain as shown in the (17). However, the phase decreases as the frequency increases.

Fig. 16 shows operating waveform of control circuit. The voltage that the switching pulse v_{CP} references to the vertical line of left, the other voltages reference to the vertical line of right. Focus on the operating waveform $|v_{\mathrm{cr\_ac}}|$ of the absolute value circuit. The absolute value circuit distorts the output voltage $|v_{\mathrm{cr\_ac}}|$ when rectifying the resonant capacitor voltage v_{cr}. This distortion causes the delay. The output of the absolute value circuit includes a low-pass filter. The circuit works as a countermeasure against comparator chattering. The output voltage $|v_{\mathrm{cr\_ac\_pass}}|$ is out of phase compared to the input voltage $v_{\mathrm{cr\_ac}}$ due to the presence of this low-pass filter. Experimental results indicate that the delay is about 0.2 μs. In this experiment, the total delay is 0.55 μs due to setting the dead time to 0.25 μs.

C. The open-loop characteristic of actual proposed method circuit

1) Heavy load: Fig. 17(a) shows the open-loop characteristic of actual proposed method circuit. The input voltage is set to 10 V. This experiment varies the load from 2 Ω to 4 Ω. This test aims to verify the operation on the actual circuit by varying the load what state the resonant capacitor voltage with a sinusoidal waveform.

The upper part of Fig. 17(a) shows the gain versus frequency, and the lower part shows the phase versus frequency. The results indicate that the control characteristics change minimally as the load varies. The gain starts to drop at around 1kHz, determined by the resonant inductor L_{r} and output capacitor C_{o}. Therefore, as shown in the Fig. 17(a), the point where the gain begins to fall remains unchanged even if the load fluctuates.

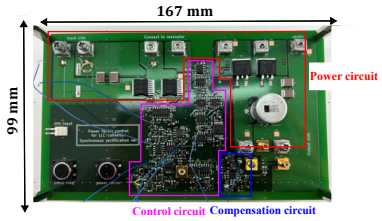

Fig. 15. Implement of LC series resonant converter using proposed method

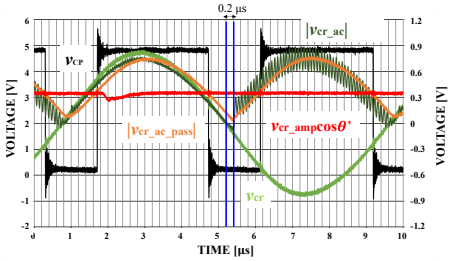

Fig. 16. Operating waveforms of control circuit

The phase of (17) consists of a combination of a secondary delay factor and a primary advance factor, so after phase is to -180 degrees, the phase eventually converges at -90 degrees. However, the phase begins to rise at around -120 degrees. This cause is primary advance factor consists of the output capacitor and the parasitic resistance. Subsequently, the phase drops again. This cause is not a characteristic of the proposed method. The amount of delay in the control circuit causes this characteristic.

2) Light load: Fig. 19 shows that the resonant capacitor voltage $v_{\rm cr}$ begins to distort from about 6 Ω. Fig. 17(b) shows open loop characteristics on light load. The input voltage is set to 18 V due to the narrow control range. light loads tend to have separated poles in control characteristics of Fig. 17(b), unlike heavy loads. Therefore, the phase characteristics does not reach -180 degrees but instead stops at -90 degrees. The phase decreases in the high-frequency region due to propagation delay effect. The results show that the plant characteristics are somewhat consistent with theoretical predictions.

The gain characteristics are nearly identical for all the different loads. The crossover frequency remains virtually unchanged. This aligns with the characteristics of the buck converter. Currently, the control range is limited due to problems within the control circuit. The proposed method will be effective even with light loads once the control circuit is improved.

D. The open-loop characteristics of previous method

Fig. 18 shows open-loop characteristics of previous method. Previous research also indicate that the result is in close agreement with the theory. The experiment result of 11 Ω deviate from the theory. The power factor control cannot be accurately represented by the equivalent circuit of Fig. 4 as the load value increases. Also, the crossover frequency is also reduced. This reduction is expected to lead to poor response

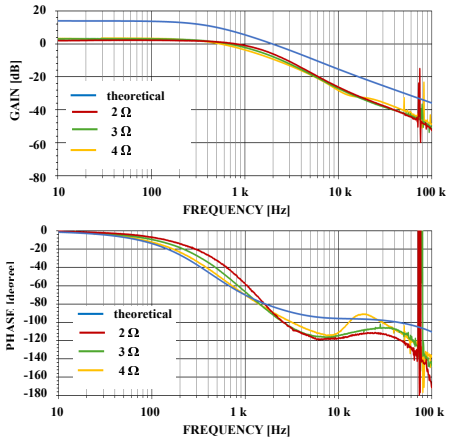

(a) Heavy load

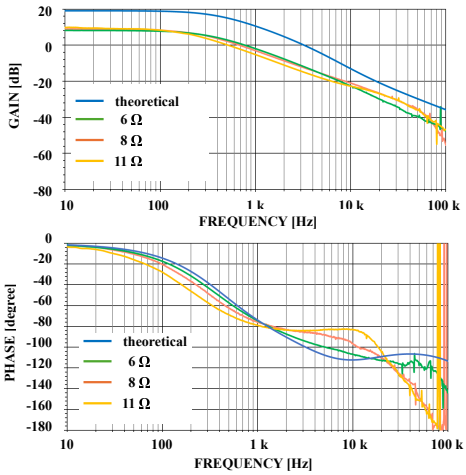

(b) Light load

Fig. 17. Open-loop characteristic of proposed method in experiment

speed at light loads. A comparison of Fig. 17 and Fig. 18 reveals similar control characteristics.

E. Load response characteristics

Fig. 20 shows load response characteristics. The undershoot is the same for both results. The two power factor controls use similar compensators. The proposed method stabilizes at approximately 12 seconds. The previous method stabilizes faster than the proposed method. This is because the crossover frequency is incorrect and the gain is low, as shown by the open-loop characteristics.

Also, The operating frequency increases as the load value increases. Hence, it difficult for the control circuit to operate properly. As a result, this slows down the load response.

V. SUMMARY

This paper described that the control characteristic does not change with load variations in LC series resonant converter using proposed method. The design of the control circuit that implements the proposed method was indicated. Then, the experimental results were evaluated by comparing to the

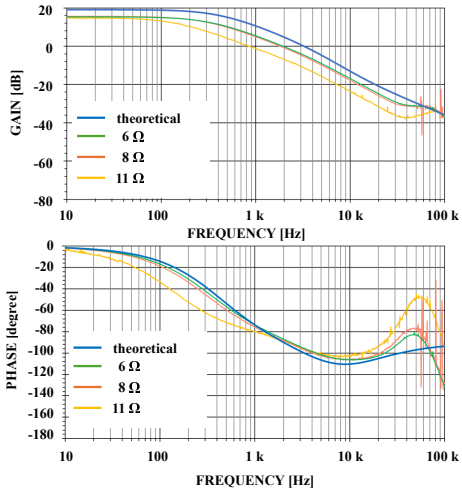

Fig. 18. Open-loop characteristic of previous method in experiment

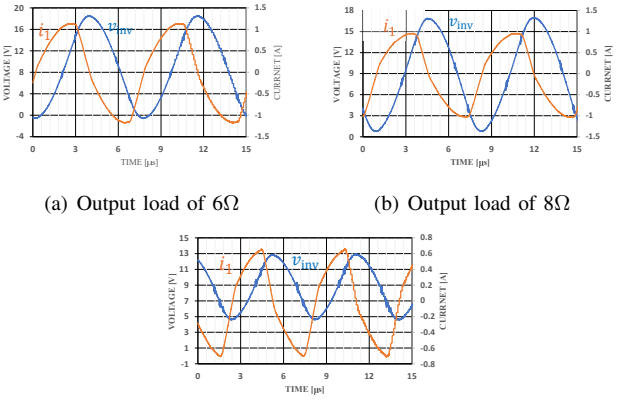

(a) Output load of 6Ω (b) Output load of 8Ω

(c) Output load of 11Ω

Fig. 19. Waveform of resonant current and voltage

theoretical characteristic (17) and previous method. As a result, the control circuit found that occurs delay. The cause of the delay was the absolute value circuit. Improvement of the circuit is in the future. The performance of the proposed method is confirmed to be equivalent to the previous studies. The small distortion rate of the waveforms in this experiment did not demonstrate the superiority of the proposed method.

In the future, The control circuit will be developed to replace the absolute value circuit. An investigation will also be conducted to examine the advantages of the proposed method over previous method.

REFERENCES

[1] A. Pratt, P. Kumar, and T. V. Aldridge, "Evaluation of 400V DC distribution in telco and data centers to improve energy efficiency," in *INTELEC 07-29th International Telecommunications Energy Conference*. IEEE, 2007, pp. 32–39.

[2] K. George and S. Ang, "Topology survey for gan-based high voltage step-down single-input multi-output dc-dc converter systems," in *2016 IEEE 4th Workshop on Wide Bandgap Power Devices and Applications (WiPDA)*. IEEE, 2016, pp. 340–343.

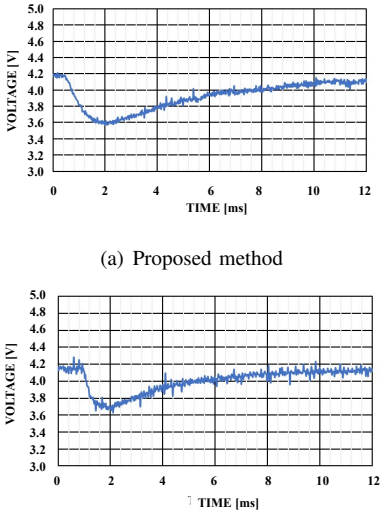

(a) Proposed method

(b) Previous method

Fig. 20. Load response of the output voltage V_o from 10 Ω to 5 Ω

[3] T. Tanaka, H. Matsumori, N. Hanaoka, K. Murai, A. Takahashi, H. Yajima, and T. Babasaki, "The HVDC power supply system implementation in NTT group and next generation power supply system," in *2014 IEEE 36th International Telecommunications Energy Conference (INTELEC)*. IEEE, 2014, pp. 1–6.

[4] J.-h. Jung and J.-g. Kwon, "Theoretical analysis and optimal design of llc resonant converter," in *2007 European Conference on Power Electronics and Applications*. IEEE, 2007, pp. 1–10.

[5] F. C. Lee, Q. Li, and A. Nabih, "High frequency resonant converters: An overview on the magnetic design and control methods," *IEEE Journal of Emerging and Selected Topics in Power Electronics*, vol. 9, no. 1, pp. 11–23, 2020.

[6] Y.-K. Tran, F. D. Freijedo, and D. Dujic, "Open-loop power sharing characteristic of a three-port resonant llc converter," *CPSS Transactions on Power Electronics and Applications*, vol. 4, no. 2, pp. 171–179, 2019.

[7] S. Tian, F. C. Lee, and Q. Li, "A simplified equivalent circuit model of series resonant converter," *IEEE Transactions on Power Electronics*, vol. 31, no. 5, pp. 3922–3931, 2015.

[8] K. Umetani, K. Shimomura, K. Yamada, T. Kawakami, M. Ishihara, and E. Hiraki, "A control method based on power factor for improving output voltage stability and efficiency of llc converter in wide range of output voltage and load impedance," in *2021 IEEE Energy Conversion Congress and Exposition (ECCE)*. IEEE, 2021, pp. 3436–3443.

[9] K. Yamada, K. Umetani, E. Hiraki, and M. Ishihara, "Phase-shift based on power factor control for llc converter with high output stability against load fluctuation," in *2022 IEEE 7th Southern Power Electronics Conference (SPEC)*. IEEE, 2022, pp. 1–6.

[10] S. Abe and T. Zaitzu, "Fundamentals of switching power supply control design," 2015 (in Japanese).

[11] S. Abe, T. Zaitzu, and T. Uematsu, *Basics and design of digital power supply : digitally controlled switch mode power supply*. Science Information Co., Ltd., July 2020 (in Japanese).

[12] K. Shimomura, K. Umetani, T. Kawakami, and E. Hiraki, *A New Control Method for Resonant Converters Based on Power Factor*. Joint Seminar on Semiconductor Power Conversion / Motor Drive, Division D, The Institute of Electrical Engineers of Japan, SPC-21-049, MD-21-049, Jan. 2021, no. 45-60 (in Japanese).